

ICEWEST-2015 [05th - 06th Feb 2015]
International Conference on Energy, Water and
Environmental Science & Technology

PG and Research Department of Chemistry, Presidency College (Autonomous),
Chennai-600 005, India

Synthesis and Characterization of ZnO Nanoparticles by Wet Chemical Method

R. Bomila¹, S. Srinivasan^{1*}

¹Department of Physics, Presidency College, Chennai- 600 005, India

Abstract: ZnO Nanoparticles were synthesized via a Wet-chemical method by using zincsulphate, Octylamine, Methanol and Sodium hydroxide. The size and morphology of the as synthesized Nanoparticles confirmed by scanning electron microscopy analysis that ZnO nanoparticles are flat, irregular in shape and having a high thickness. The X-ray diffraction (XRD) study revealed that the synthesized ZnO product has the pure wurtzite structure with lattice parameters $a=b=3.253 \text{ \AA}$ and $c=5.210 \text{ \AA}$, respectively. The average crystallite size of the ZnO nanostructures from the Scherer's formula is $\sim 34 \text{ nm}$. The FT-Raman scattering exhibits a sharp and strong E₂ mode at 449 cm^{-1} which further confirms the good crystalline and wurtzite hexagonal phase of the prepared ZnO nanostructures. The synthesized powder exhibited the UV absorption at around 370 nm with the estimated direct band gap energy of 3.43 eV .

Keywords: ZnO, Wet-Chemical synthesis, X-ray diffraction, Raman scattering, Optical Properties.

Introduction

ZnO is a wide band gap semiconductor with optoelectronic properties that make it an attractive candidate for a variety of device applications. Zinc oxide is a versatile material that has achieved applications in photo catalysts, solar cells, chemical sensors, piezoelectric transducers, transparent electrodes¹⁻³, electroluminescent devices, and ultraviolet laser diodes⁴⁻⁵. The ZnO has wide band gap of 3.37 eV and other large excitation binding energy, which makes excitation stable even at room temperature. There are various methods in order to synthesize ZnO nanomaterials viz. solvothermal synthesis, sol-gel⁶, combustion synthesis, Spray analysis, thermal hydrolysis, hydrothermal synthesis etc⁷⁻¹⁰. Hydrothermal synthesis is one of the most extensively used and cost effective methods for the preparation of nanomaterials. In this study, we have synthesized ZnO nanomaterials and their optical and surface morphological properties are investigated.

Experiments

Synthesis of ZnO nanoparticles

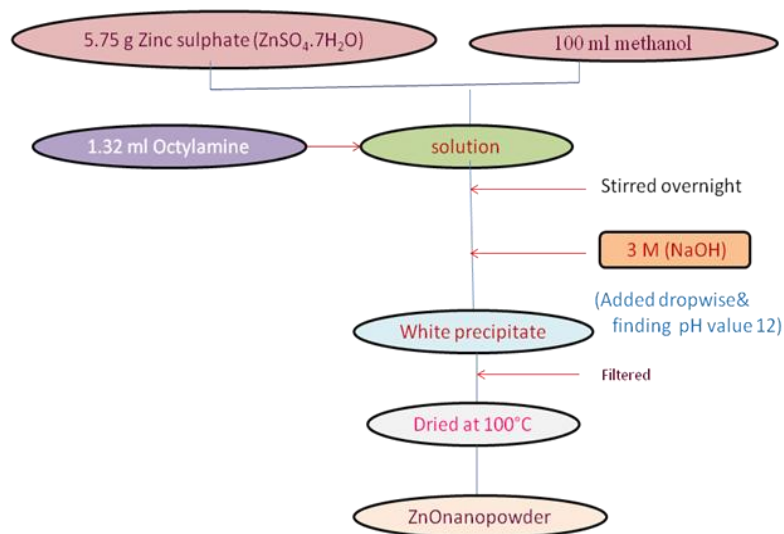


Fig 1. The Flow chart showing the procedure for ZnO nanoparticles

Zinc oxide was synthesized in aqueous solutions by using Zinc sulphate, Methanol, sodium hydroxide and octylamine. 5.75g of zinc sulphate (AR) is taken in a beaker containing 100ml of methanol(AR) and 1.32 ml of octylamine and stirred for about 24 h. 3M sodium hydroxide is added drop wise to change the pH value up to 12. White precipitates thus obtained are filtered and washed with methanol and distilled water to remove impurities and dried over 100°C for 6 hrs in order to remove water molecules. The synthesized procedure is depicted in Fig.1.

Material Characterization

The synthesized ZnO nanoparticles characterized for their structure and morphology by XRD and SEM. The XRD patterns of the powdered samples were recorded using a Bruker D8 Advanced X-ray diffractometer (BrukerOptik GmbH, Ettlingen, Germany) with CuK α radiation ($\lambda = 1.5418 \text{ \AA}$, rated as 1.6 kW) radiation and scanning range of 2θ set between 20° to 80° and SEM images of the samples were taken using a Philips XL 30 ESEM scanning electron microscope (FEI-Philips Company, Hillsboro).

The UV–Vis absorption spectra of the samples were recorded in the wavelength range of 190 to 800 nm using a Shimadzu UV 3600 UV–Vis-NIR spectrometer (Shimadzu Corporation, Kyoto, Japan) in diffuse reflectance mode using BaSO₄ as reference. Spectra were recorded at room temperature, and the data were transformed through the Kubelka-Munk function. FT-RAMAN spectra were recorded using Perkin Elmer RX1 Model FT-RAMAN spectrophotometer in the range between 4000 to 400 cm⁻¹.

Results and Discussion

Structural properties

The powder XRD pattern of Octylamine – stabilized ZnO nanoparticles were shown in Figure 2. All the diffraction peaks are well indexed to the hexagonal ZnO wurtzite structure (JCPDS Card no. 36–1451). Diffraction peaks corresponding to the impurity were not found in the XRD patterns, confirming the high purity of the synthesized products. A definite line broadening of diffraction peaks indicates that the synthesized materials are in the nanometer range.

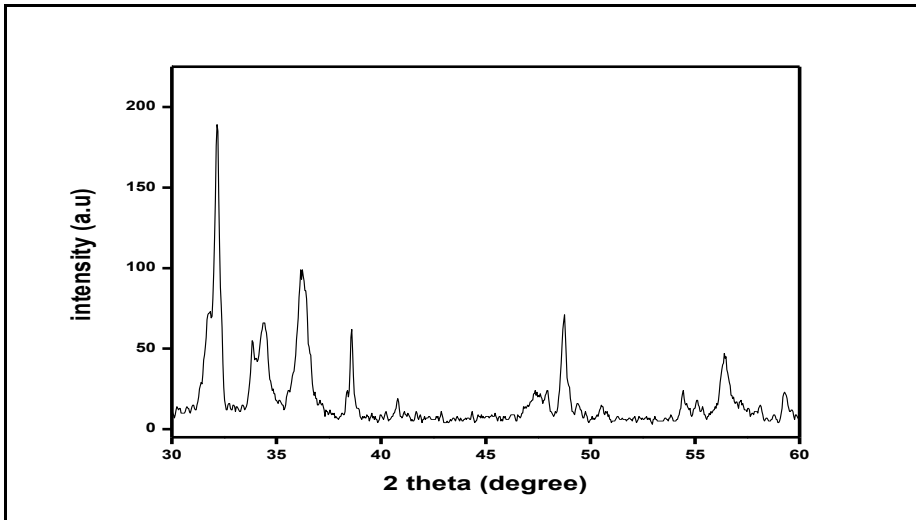


Fig. 2 XRD patterns of ZnO power

Table 1 shows the average crystallite sizes of the samples calculated by Debye-Scherrer's equation (Equation 1) using the full width at half maximum of the X-ray diffraction peaks. The average crystallite size is found to be 34 nm. At such high temperatures, migration of grain boundaries occurs, causing the coalescence of small grains and formation of large grains.

$$D = \frac{0.89\lambda}{\beta \cos\theta} \dots\dots (1)$$

where D is the crystallite size (nm), λ is the wavelength of incident X-ray (nm), β is the full width at half maximum, and θ is the diffraction angle.

Table 1. Particle size of ZnO

S.No	2 θ	hkl	FWHM	Size of the particle (nm)
1	32.163	100	0.24	34.12
2	34.398	002	0.24	34.32
3	36.217	101	0.24	34.5
4	48.735	102	0.16	53.93
5	56.411	110	0.24	37.21
6	62.62	103	0.24	38.38
7	67.641	112	0.24	39.47

SEM analysis

The SEM images of the samples were shown in Figure 3. The SEM images of ZnO samples show that the agglomerations of particles are much less in this method of preparation. The SEM images of ZnO at room temperature show the presence of nanoparticles. The energy dispersive spectra of the samples obtained from the SEM-EDS analysis clearly show that the sample prepared by the above route has pure ZnO phases.

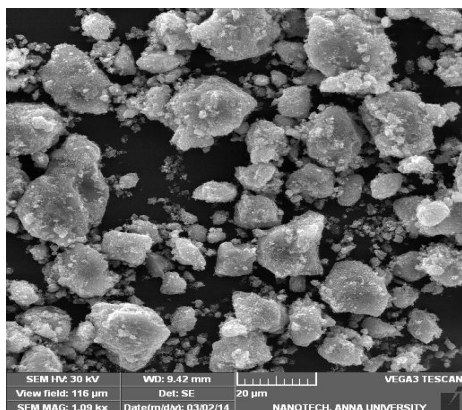


Fig. 3 SEM image of ZnO Nanoparticles

Raman Spectroscopy

The Raman-scattering spectra of the as grown ZnO structures are shown in Figure 4. With 532 nm laser light (Nd:YAG) laser as an excitation source. The Raman signals are usually very sensitive to the structure of crystal as well as to the defects in the crystal structure. The crystal structure of ZnO is wurtzite (hexagonal) which belongs to the $4\ 6v\ C$ space group having two formula units per primitive cell with all the atoms occupying the $C3v$ sites. According to Group theory, there are eight sets of zone centre optical phonons, where A1 and E1 modes are polar which split into transverse optical (A1T and E1T) and longitudinal-optical (A1L and E1L) phonons, while the E2 mode consists of two modes of low- and high-frequency phonons (E2L and E2H) which are Raman-active. The main dominant sharp peak labeled as E2 at 437 cm^{-1} was observed and is known as Raman active optical phonon mode, which is the characteristic of wurtzite hexagonal phase ZnO. Other peaks are also usually observed, i.e. the peak at $\sim 98\text{ cm}^{-1}$ known as E2(Low), and the peak at 339 cm^{-1} is the second-order Raman spectrum, originating from the zone boundary phonons $3E2H-E2L$ and the peak at 388 cm^{-1} can be labeled as A1T. The relatively higher intensity and sharp peak of E2 mode at 437 cm^{-1} compared to the other observed peaks, demonstrated that the as-grown ZnO structures are of wurtzite hexagonal phase with good crystallinity. Table 2. gives a comparison of the Raman peak with the theoretical values reported by ¹¹.

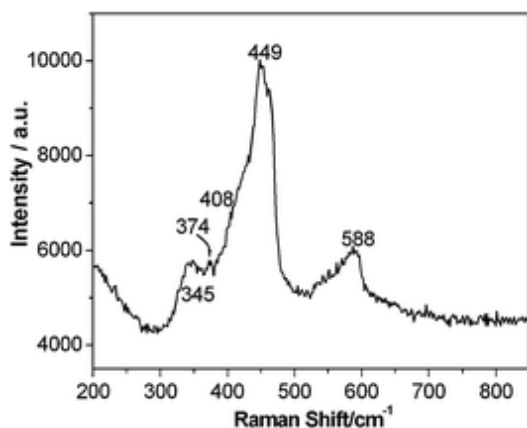


Fig. 4. FT-Raman spectrum of ZnO Nanoparticles

Table 2. Comparison of FT-Raman spectral values of ZnO

Symmetry	Theoretical ⁽¹¹⁾ wavenumber (cm^{-1})	Observed wavenumber (cm^{-1})
E2 (Low)	99	-
A1(TO)	378	374
E1(TO)	403	408
E2(High)	435	449
A1(LO)	571	-
E1(LO)	580	588

Diffuse reflectance analysis

The UV-visible absorption spectra of the samples are shown in Figure 5.(A, B) atypical excitation absorption at 370 nm is observed in the absorption spectrum at room temperature, which is shifted with respect to the bulk absorption edge appearing at 380 nm at room temperature. It is clear that the absorption edge systematically shifts to the lower wavelength or higher energy with decreasing size of the nanoparticles. This pronounced and systematic shift in the absorption edge is due to the quantum size effect. The band gap energy of the samples are measured by the extrapolation of the linear portion of the graph between the modified Kubelka-Munk function $[\alpha hv]^2$ versus photon energy (hv). The extrapolating the linear portion of the curve to absorption equal to zero gives the value of the direct band gap to be 3.4 eV. This value is higher than that of 3.3 eV reported in the literature. Band gap energy increases with decreasing particle size due to quantum size effects.

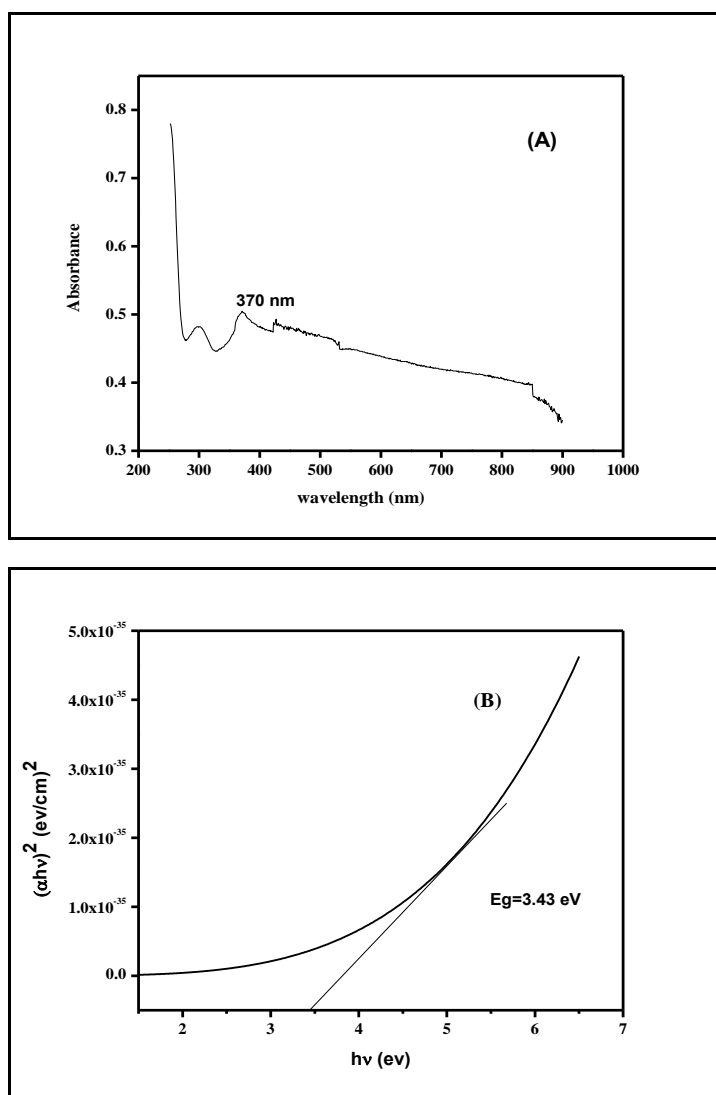


Fig. 5(A)UV-Visible spectrum of ZnO and(B) Tauc's plot of ZnO

Conclusion

ZnO nanoparticles were prepared using a simple wet chemical method. The effect of ligand stabilized on the growth of ZnO nanoparticles has been investigated experimentally. This work provides a simple and efficient way to control the size of ZnO nanoparticles. The powder-XRD studies revealed that the particles are nanocrystalline in nature with grain size around 53 nm to 34 nm for with ligand nanoparticles. SEM images of the ZnO powder showed that the nanoparticles are homogeneous with size for with ligand respectively. From the UV-Vis spectra, the Band gap energy were calculated to be 3.43 eV with ligand ZnO nanoparticles respectively. The observed peak at 449 cm^{-1} is due to Raman active it confirmed the wurtzite hexagonal phase of particle.

References

1. Chakrabarti S, Dutta B. K., Photo catalytic Degradation of Model Textile Dyes in Wastewater Using ZnO as Semiconductor Catalyst, *Journal of Hazardous Materials*, 2004, 112 : 3:269-278.
2. Shishiyanu T. S, Lupen O. I., Sensing Characteristics of Tin-Doped ZnO Thin Films as NO₂ Gas Sensor, *Sensors and Actuators B: Chemical*, 2005, 107: 1: 379-386.
3. Suvaci E, Ozer I. O., Processing of Textured Zinc Oxide Varistors via Templated Grain Growth, *Journal of the European Ceramic Society*, 2005, 25: 9: 1663-1673.
4. Saito N, Haneda H, Sekiguchi T, Ohashi N, Sakaguchi I, Koumoto K., Low-Temperature Fabrication of Light-Emitting Zinc Oxide Micropatterns Using Self-Assembled Monolayers, *Advanced Materials*, 2002, 14: 6: 418-421.
5. Meron T, Markovich G., Ferromagnetism in Colloidal Mn²⁺-Doped ZnO Nanocrystals, *Journal of Physical Chemistry B*, 2005, 109: 43: 20232-20236.
6. Luna-Arredondo E. J, Maldonado A, Asomoza R, Acosta D. R, Melendez-Lira M. A., Indium-Doped ZnO Thin Films Deposited by the Sol- Gel Technique, 2005, 490: 2:132-136.
7. Xu CX, Sun XW, Dong ZL, Cui YP, Wang BP., Nanostructured single crystalline in disks of zinc oxide *Crystal Growth & Design* 2007, 5:41-44.
8. Natsume Y, Sakata H., Electrical and Optical Properties of Zinc Oxide Films Post-Annealed in H₂ after Fabrication by Sol-Gel Process, *Materials Chemistry and Physics*, 2002, 78:1: 170-176.
9. Deenathayalan J, Saroja M, Venkatachalam M, Gowthaman P, Senthil T.S., Effect of Growth layer solution concentration on the structural and optical properties of hydrothermally grown Zinc Oxide nano rods, *Chalcogenide letters*, (2011), 8:9:549 –554
10. Deenathayalan J, Saroja M, Venkatachalam M, Gowthaman P, Senthil T.S, Shankar S., Fabrication of natural dye sensitized solar cell using hydrothermally grown zinc oxide nanorod, *International Journal of Nano science and Nanotechnology*, 2012, 3 :2:81-89
11. Shah A.H, Manikandan E, Basheer Ahamed M, Dilawar Ahmad Mir, Sajad Ahmad Mir., Antibacterial and Blue shift investigations in sol-gel synthesized Cr_xZn_{1-x}O Nanostructures *Journal of luminescence* (2014), 145:944-950.
